Journal of Biological Physics **29:** 187–194, 2003.

On-Chip THz Detection of Biomaterials: A Numerical Study

T. BARAS, T. KLEINE-OSTMANN* and M. KOCH
Institut für Hochfrequenztechnik, Technische Universität Braunschweig Schleinitzstrasse 22 – 38106 Braunschweig, Germany
(**Author for correspondence, e-mail: t.kleine-ostmann@tu-bs.de*)

Abstract. The marker-free on-chip distinction between hybridised (double-stranded) DNA (HDNA) and denatured (single-stranded) DNA (DDNA) has recently been demonstrated using ultrashort electrical pulses. The electrical THz pulses propagate in integrated waveguides incorporating resonant THz structures onto which the genetic material is deposited. For a possible future realisation of a high throughput array, it is crucial to optimize the experimental parameters and the resonant structure. In this paper we perform a first numerical study of different resonator geometries and examine the influence of critical experimental parameters on the transmission characteristics of the resonant structures. Our simulations demonstrate that the ring resonator shows a comparable performance to the parallel-coupled resonator previously used in a first demonstration by Nagel and coworkers.

Key words: lab-on-chip, marker-free DNA testing, numerical simulations, on-chip DNA analysis, parallel-coupled filter, ring resonator, THz on-chip detection, THz spectroscopy

1. Introduction

The market potential of methods for rapid identification of genetic sequences is tremendous. Most current techniques are based on fluorescent labelling [1] of the denatured target DNA molecules in which a known base sequence has to be identified. Such labelling presents an additional preparation step. It does not only restrict the sample processing speed and cost-effectiveness but might also affect the DNA strand conformation, hence lowering the yield and the reliability of the method [2].

Hence, a marker-free detection method would be highly welcome. Recently Brucherseifer et al. demonstrated an approach using electrical THz pulses that propagate along thin-film microstrip lines [3]. These structures incorporate a resonant structure which is detuned when loaded with genetic material. The DNA is deposited simply by pipetting it from an aqueous solution onto the resonant structure. After water evaporation the DNA forms a thin film with a thickness of only a few tens of nanometers. The train of electrical THz pulse is generated using a Ti:Sapphire laser with a repetition rate of 78 MHz. The laser pulses gate a biased photoconductive switch which causes an electric signal to propagate along the microstrip line and through the DNA-loaded parallel-coupled quarter-wavelength mi-

crostrip line resonator. The transmitted pulses are detected via electro-optic sampling [4].

In their pioneering and impressive work Nagel et al. demonstrated that they could determine the state of hybridisation of small samples of nucleic acids down to a femtomol level [3]. Their system truly holds a high potential for the development of marker-free high-throughput genetic diagnostic instruments.

In this paper we perform a numerical study of different resonator geometries using commercially available simulation packages. Firstly, we examine the structure employed by Nagel et al.. Secondly, we explore a ring resonator as an alternative structure for on-chip THz analysis of biomolecules. We find, that the shift of the resonance frequency is higher for HDNA than for DDNA. For both materials the frequency shift saturates above a DNA layer thickness of 20 to 25 μm. Altogether, the performance of the ring resonator is comparable to that of the parallel-coupled quarter-wavelength microstrip line resonator.

2. Simulation Tools

Two different commercial simulation packages are used to calculate and design the characteristics of microstrip line filter structures. Serenade^{TM} from Ansoft allows a user to set up a filter structure from discrete elements and simulate it over the desired frequency range. Each microstrip line element is characterised by its impedance and electrical length. The program uses the transmission line equations to calculate a set of parameters for the given structure. From this the scattering parameters of the structure are deduced. The program does not account for radiation losses which become quite important at a few hundred GHz. Yet, since calculations with this program do not take longer than a few seconds, it is perfectly suited for a quick rough filter design which matches the desired resonance frequency.

In order to account for the lost power that is radiated from the filter structure and to be able to simulate a target DNA load as dielectric layer on top of our structure, we use the simulation tool Momentum^{TM} which is part of the design environment Advanced Design System (ADS)^{TM} from Agilent Technologies. It uses the method of moments which is based on a numerical solution of the integral equation which connects the radiated electric field with the current distribution of a given structure via Green's function. Discretisation of the currents yields a linear system of equations. Momentum^{TM} does not take modes of higher order into consideration. Hence, only sufficiently thin substrates will be simulated correctly. At a reasonable substrate height of 20 μm we expect single mode operation up to approximately 1 THz, the estimated cut-off frequency for the first higher mode.

3. Results and Discussion

First, we examine the transmission characteristics of the parallel-coupled quarter-wavelength microstrip line resonator shown in Figure 1. We tried to get the design

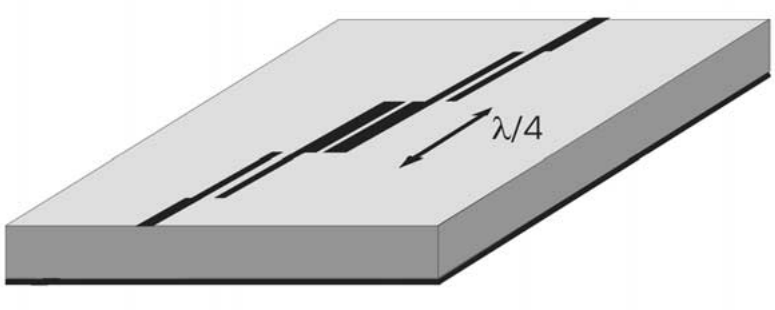

Figure 1. Geometry of a parallel-coupled quarter-wavelength microstrip line resonator.

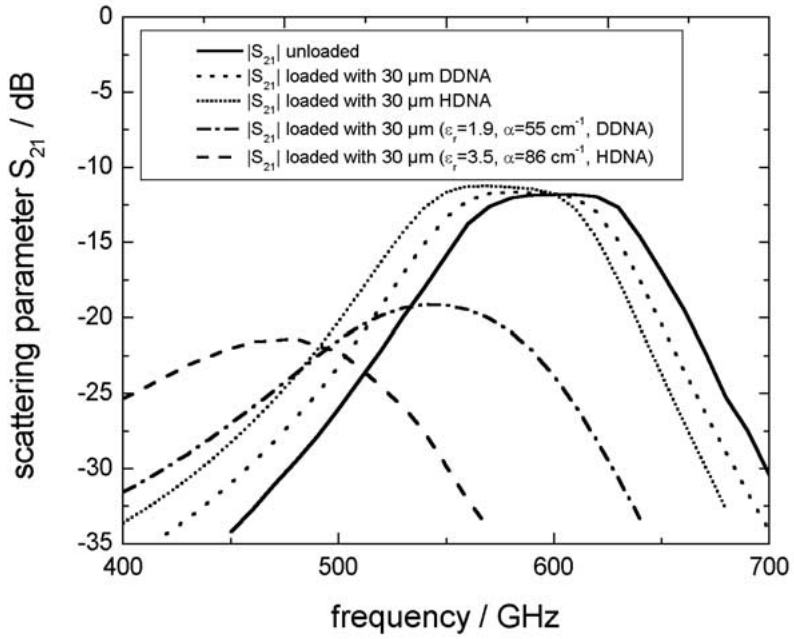

Figure 2. Scattering parameter S_{21} calculated for the parallel-coupled quarter-wavelength microstrip line resonator of Figure 1. (solid line: unloaded, short dashed: loaded with 30 μm dry DDNA, short dotted: loaded with 30 μm dry HDNA, dash-dotted: loaded with 30 μm DNA assuming $\varepsilon_r = 1.9$, $\alpha = 55$ cm^{-1}, DDNA, long dashed: loaded with 30 μm DNA assuming $\varepsilon_r = 3.5$, $\alpha = 86$ cm^{-1}, HDNA).

of the structure as close as possible to the one described by Nagel et al. [3]. The coupling length is $\lambda/4$ for a design wavelength of 610 GHz and a substrate thickness of 6 μm benzocyclobutene (BCB). The parallel-coupled filter is supposed to have a transmission maximum at its resonance frequency.

Figure 2 shows a Momentum^{TM} simulation of the scattering parameter S_{21}. A passband centred around 600 GHz is clearly visible for the unloaded structure

(solid line). The simulation hence reproduces the main features observed experimentally in [3]. In order to also reproduce the tremendous resonance frequency shifts measured by Nagel et al. of 50 GHz (8%) for the structure loaded with DDNA and of 130 GHz (21%) for the structure loaded with HDNA, we perform calculations assuming dielectric layers of 80 nm thickness. The resonance curve does not shift distinctively if one chooses $\varepsilon_r = 1.44$ for HDNA and an absorption constant of $\alpha = 10\ \mathrm{cm}^{-1}$, taking into account possible dielectric losses of DNA [5] (not shown). Even a 80 nm water layer with $\varepsilon_r = 5$ and $\alpha = 170\ \mathrm{cm}^{-1}$ does not change the transmission characteristics significantly (not shown). Altogether we were not able to numerically confirm the large frequency shifts observed experimentally in [3] with DNA layers with a thickness of only a few tens of nanometers.

The large frequency shifts are also not reproduced with thick layers of dry DNA. The short dashed and short dotted lines in Figure 2 show the simulation results for films of 30 μm DDNA and 30 μm HDNA, respectively. Now the resonance frequency shift is approximately 20 GHz (3%) for DDNA and 30 GHz (5%) for HDNA. DDNA and HDNA can, however, clearly be distinguished. It is yet not possible to increase the frequency shift any further by increasing the DNA layer thickness. Hence, we increased the dielectric constant of the simulated DNA layer in order to obtain the frequency shifts and amplitudes measured in [3]. The long dashed and dash-dotted lines in Figure 2 show that at a dielectric constant of $\varepsilon_r = 1.9$ for DDNA and $\varepsilon_r = 3.5$ for HDNA and a serious absorption is necessary to cause these resonance frequency shifts at a simulated layer thickness of 30 μm.

Of course, the question arises: what could be the origin for the discrepancy between the experimental results by Nagel et al. and this numerical study? A possible explanation would be that the DNA samples on top of the filter structure in [3] were much thicker than stated and were also not completely dry ($\alpha \gg 10\ \mathrm{cm}^{-1}$) when measured. However, the authors claim that they are very certain about these parameters [6].

Since we are certain that the simulation software works properly at THz frequencies [7] the discrepancy remains puzzling. Also, the simulations were stable. The same resonator geometry always resulted in the same scattering parameters. Yet, we can not finally exclude that we did not match the Nagel structure exactly (although we tried our very best) and that a structure which is only slightly different leads to completely different results. To explore the sensitivity of the filter characteristics to changes in the filter geometry we performed calculations for other slightly different unloaded structures. As can be seen in Figure 3 (line a) a more simple filter design with three equal $\lambda/4$ couplers leads to a less pronounced resonance with a shallow dip. The overall characteristics are not too strikingly different though. The superior Nagel structure (line b), however, appears to be quite insensitive to geometrical deviations as they might occur once large throughput arrays are made. We simulated this by adding a triangular shaped perturbance to the third coupler (line c).

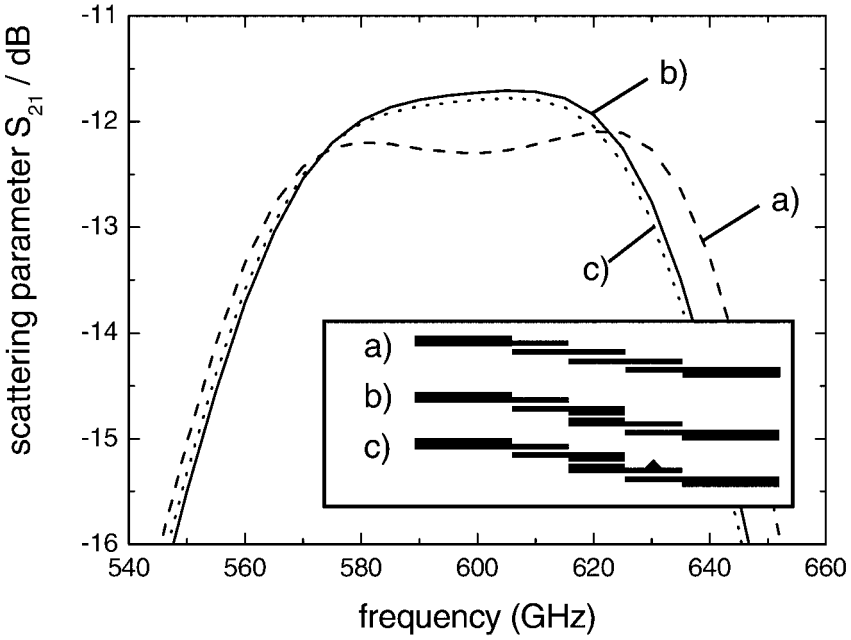

Figure 3. Scattering parameter S_{21} calculated for the parallel-coupled quarter-wavelength microstrip line resonator for different geometry variations. (dashed line: first simple approach, solid: improved design, dotted: design with triangular perturbance).

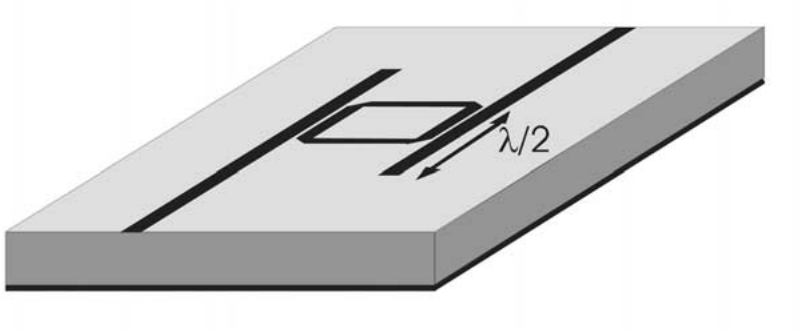

Figure 4. Geometry of a ring resonator.

Alternatively, one can imagine that there are physical effects involved that are not included in the simulation software, e.g., that a thin layer of DNA for some reason shows a distinct AC conductance leading to higher values of the dielectric constant (a somewhat conductive layer on top of the resonator would not be properly included in the program). However, such a conductance has not been observed yet experimentally [5,8] and remains pure speculation at the moment.

Despite the fact that we were not able to numerically confirm the large frequency shifts observed in [3] we can explore other resonator geometries and com-

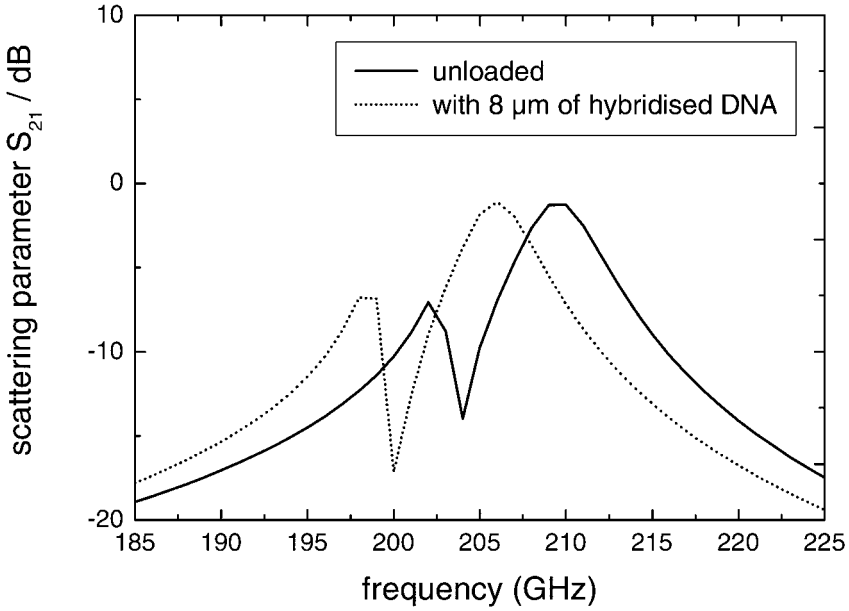

Figure 5. Scattering parameter S_{21} calculated for the ring resonator of Figure 3. (solid line: unloaded, dotted: loaded with 8 μm dry HDNA).

pare their performance with the parallel-coupled quarter-wavelength microstrip line resonator. In the following we perform a first examination of a ring resonator, the geometry of which is shown in Figure 4. Due to the closed shape of the ring resonator, we can expect significantly reduced radiative losses as compared to structures like a quarter-wavelength shunt-stub bandstop filter. The structure in Figure 4 has a side length of $\lambda/4$ at a resonance frequency of 220 GHz and quarter-wavelength stubs to enhance coupling into the ring. The thickness of the BCB substrate is 20 μm in this case. The transmission characteristics of this structure show a distinct resonance (Figure 5, solid line). An additional load of HDNA (ε_r = 1.44, no losses) shifts the resonance frequency towards lower values. The dashed line in Figure 5 is obtained for a load of 8 μm dry HDNA and shows a frequency shift in the transmission factor S_{21} of 4 GHz (2%). This is comparable but somewhat less than the shift found for the parallel-coupled quarter-wavelength microstrip line resonator.

With the ring resonator structure we more closely examine how the resonance frequency shift depends on the layer thickness and the hybridisation state of the DNA sample. Figure 6 shows the resonance frequency as a function of sample thickness for dry HDNA (ε_r = 1.44, no losses) and dry DDNA (ε_r = 1.21, no losses). From this numerical study we can conclude that the sample thickness should be above 10 μm in order to obtain a maximum difference in the resonance frequencies and, hence, to permit a reliable distinction between both types of DNA.

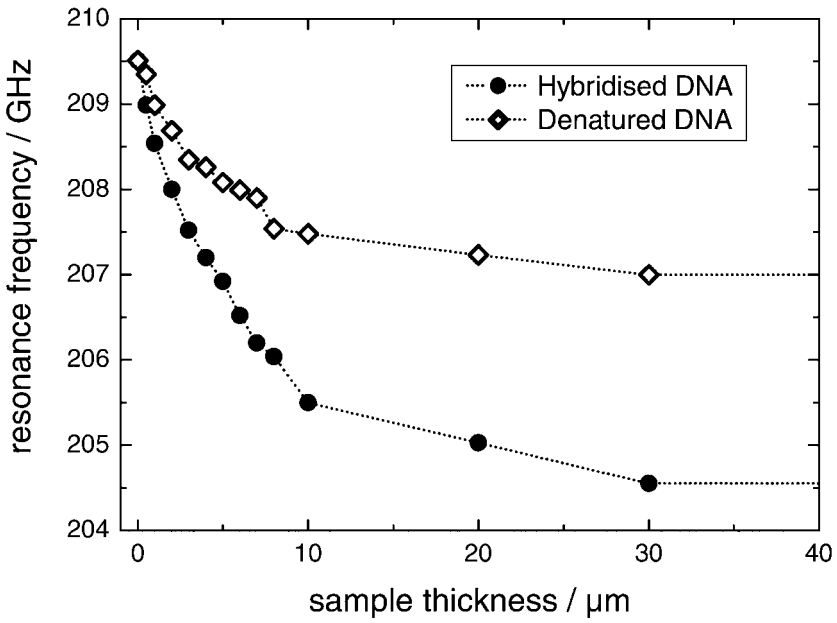

Figure 6. Resonance frequency of the ring resonator structure vs. DNA sample thickness.

Furthermore, the maximum tolerance in layer thickness fluctuations for a given nominal layer thickness can be estimated. For instance, at a nominal layer thickness of 20 μm, the fluctuation should not exceed 10 μm.

4. Conclusion

In this paper we have performed a numerical study of the performance of resonator geometries that could be used for on-chip THz detection of genetic material. We used Momentum^{TM} to examine the parallel-coupled microstrip line resonator used in [3] and a ring resonator. While it remains unclear why the large frequency shift observed by Nagel et al. can not be reproduced numerically with very thin films of DNA we can conclude from our simulations that a ring resonator shows a comparable performance to the parallel-coupled resonator. We determine a minimum layer thickness for reliable DNA detection.

References

1. Chee, M., Yang, R., Hubbell, E., Berno, A., Huang, X.C., Stern, D., Winkler, J., Lockhart, D.J., Morris, M.S. and Fodor, S.P.A.: Accessing Genetic Information with High-Density DNA Arrays, *Science* **274** (1996), 610–614.
2. Zhu, Z., Chao, J., Yu, H. and Waggoner, A.S.: Directly labeled DNA Probes using Fluorescent Nucleotides with Different Length Linkers, *Nucl. Acids Res.* **22** (1994), 3418–3422.

3. Nagel, M., Haring Bolivar, P., Brucherseifer, M., Kurz, H., Bosserhoff, A. and Büttner, R.: Integrated THz Technology for Label-Free Genetic Diagnostics, *Appl. Phys. Lett.* **80** (2002), 154–156.
4. Valdmanis, J.A. and Mourou, G.A.: Subpicosecond Electrooptic Sampling: Principles and Applications, *IEEE J. Quant. Electr.* **22** (1986), 69–78.
5. Markelz, A.G., Roitberg, A. and Heilweil, E.J.: Pulsed Terahertz Spectroscopy of DNA, Bovine Serum Albumin and Collagen between 0.1 and 2.0 THz, *Chem. Phys. Lett.* **320** (2000), 42–48.
6. Haring Bolivar, P.: private communication.
7. The simulation program is scalable and there is no obvious reason why it should not work at THz frequencies. We will cross-validate this, however, in the next future by using alternative simulation software from other providers.
8. Brucherseifer, M., Nagel, M., Haring Bolivar, P., Kurz, H., Bosserhoff, A. and Büttner, R.: Label-Free Probing of the Binding State of DNA by Time-Domain Terahertz Sensing, *Appl. Phys. Lett.* **77** (2000), 4049–4051.